Electronic Supplementary Material ESM 2

Polybaric fractional crystallisation of arc magmas: an experimental study simulating trans-crustal magmatic systems

Felix Marxer[1,2*], Peter Ulmer[1], Othmar Müntener[3]

[1]*Institute of Geochemistry and Petrology, ETH Zürich, Clausiusstrasse 25, 8092 Zürich, Switzerland*

[2]*Institute of Mineralogy, Leibniz University Hannover, Callinstraße 3, 30167 Hannover, Germany*

[3]*Institute of Earth Sciences (ISTE), University of Lausanne, Bâtiment Géopolis, 1015 Lausanne, Switzerland*

**Corresponding author:*

E-Mail: f.marxer@mineralogie.uni-hannover.de

Information

This Electronic Supplementary Material ESM 2 contains additional figures illustrating the employed experimental approaches as well as information on supplemental measurements of residual melt water contents determined by Raman spectroscopy not presented in the main part of the paper.

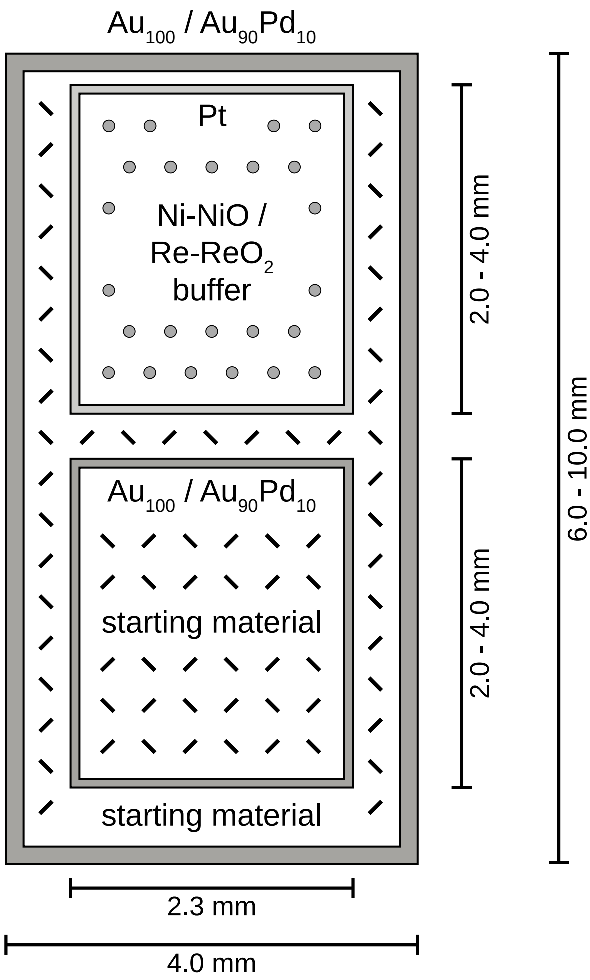

Figure ESM2.1: Capsule design used in this study representing a modification and combination of the setups after Kaegi et al. (2005) and Matjuschkin et al. (2015). Two inner capsules with an outer diameter (OD) of 2.3 mm containing the experimental charge and the solid fO_2 buffer assemblage are positioned in a larger outer capsule (4.0 mm OD) containing the same starting material as the inner capsule as spacer material.

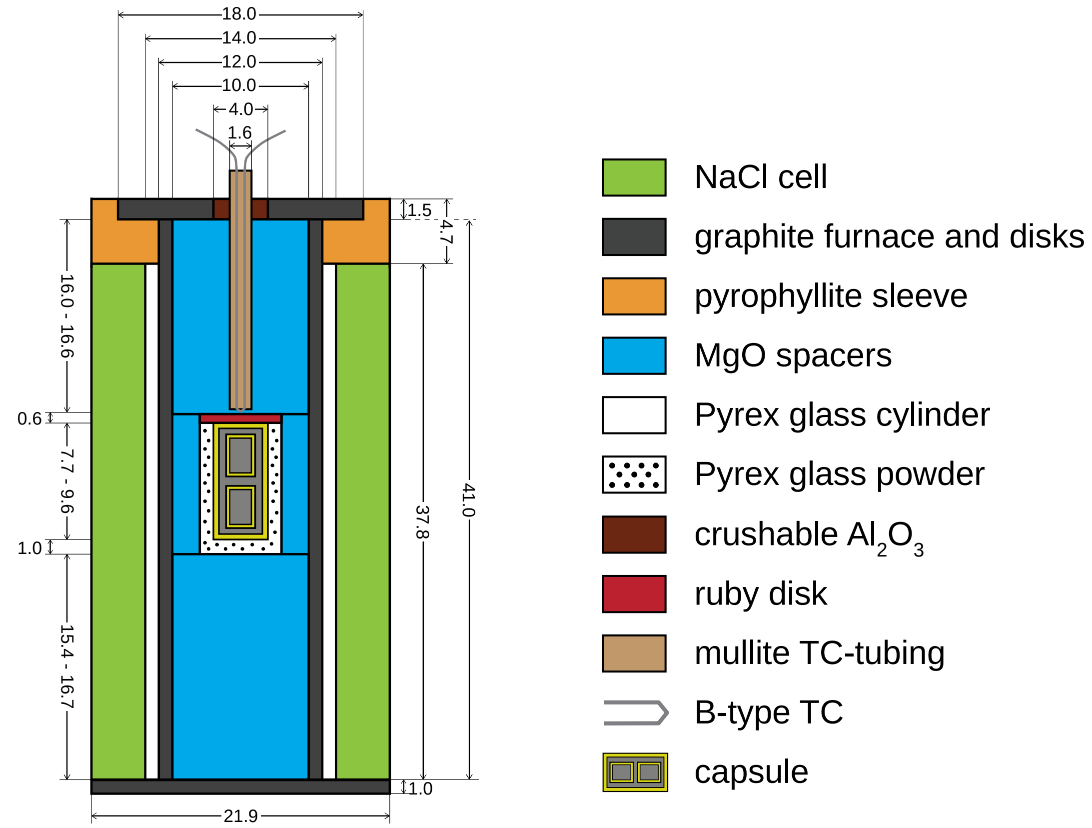

Figure ESM2.2: 22-mm assembly for experiments at 0.4 GPa in the non-end-loaded Johannes-type piston cylinder. Dimensions are given in mm.

Water contents of residual glasses determined by Raman spectroscopy

Melt water contents of selected runs were measured by Raman spectroscopy at KU Leuven (Belgium) using a Horiba LabRAM HR Evolution System. Samples were excited with a Nd:YAG laser with a wavelength of 532 nm and a grating of 1800-groove/mm was applied. Analysis were performed with a 100x magnification objective corresponding to a laser spot size less than 1.5 µm. Measurements were done with a pinhole aperture of 50 µm over a spectral window from 50 to 4000 cm^{-1}. Acquisition times varied between 50 to 200 s per frame with two accumulations, and a spike filter was applied to remove any non-repetitive spikes. Laser energy was varied between 100 and 25 % to avoid any damage of the sample influencing the signal quality. Raw spectra were processed following the approach of Le Losq et al. (2012). Water contents were quantified employing an in-house linear calibration established by T. van Gerve and O. Namur (van Gerve et al. 2021) based on various well-characterised water-bearing standard glasses where the area ratio between the high-wavenumber OH band (3000-4000 cm^{-1}) and the low-wavenumber silicate bands (15-1500 cm^{-1}) is related to the melt water content (in wt.%).

Measured water contents (in wt.%) are reported in Table ESM2.1 and plotted versus nominal melt water contents established via mass balance (compare Table 2) in Figure ESM2.3. Generally, Raman and nominal water contents both exhibit an identical evolution of persistently increasing values upon differentiation (i.e. decreasing temperature). In detail, for most experiments, Raman data and nominal water contents agree well (within 0.5 wt.%). Higher deviations for high-temperature runs with lowest nominal H_2O concentrations (e.g. FM40 or FM157) can be explained by pronounced Fe-loss and H-diffusion into inner experimental capsules resulting in additional water formation in these charges. The overestimation of melt water content via Raman for the experiment with the

Table ESM2.1: Water contents (in wt.%) of experimental glasses derived by mass balance calculation and measured with Raman spectroscopy.

Run	Pressure (GPa)	Temperature (°C)	nominal H_2O (wt.%)	Raman H_2O (wt.%)	σ
hot path					
FM40	0.8	1110	3.53	4.64	0.16
FM93	0.6	1050	4.60	5.06	0.16
FM127	0.4	1020	4.62	4.62	0.09
FM129	0.4	990	5.60	5.19	0.13
hot oxidised path					
FM134	0.6	1050	4.39	4.46	0.14
hot rk52 path					
FM157	0.6	1050	4.08	5.12	0.02
intermediate path					
FM112	0.6	1020	4.74	4.68	0.10
FM128	0.4	960	6.62	7.14	0.26
cold path					
FM116	0.6	960	6.33	6.62	0.28
FM145	0.4	870	9.05	10.53	0.64

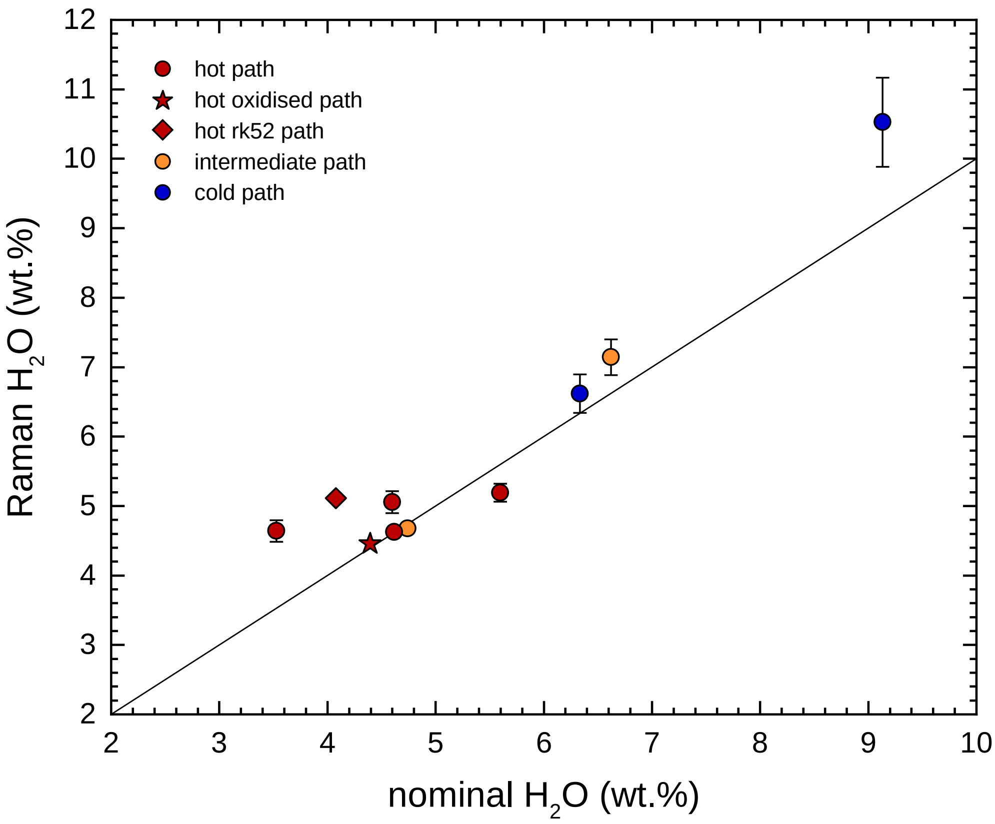

Figure ESM2.3: Nominal melt water contents (in wt.%) established via mass balance calculations compared with water contents (wt.%) measured with Raman spectroscopy. The black line illustrates a 1:1 trajectory. In cases where error bars are not shown their extent is smaller than the symbol size.

highest nominal H_2O (FM145, 10.53 vs 9.05 wt.%) could be related to the extrapolation of the calibration to such high water contents as that high H_2O concentrations were not covered by the glass standards used for calibration. Alternatively, the nominal water content of this experiment (that reached water-saturation) could have been slightly underestimated due to uncertainties on MagmaSat calculations. In fact, ignoring the potential attainment of water-saturation (as inferred from MagmaSat), the estimated nominal melt water content based on mass balance (10.57 wt.%) perfectly agrees with the Raman data.

Acknowledgements

Thomas van Gerve and Olivier Namur are gratefully acknowledged for their hospitality and assistance during Raman measurements at KU Leuven.

References

Kaegi R, Muentener O, Ulmer P, Ottolini L (2005) Piston-cylinder experiments on H_2O undersaturated Fe-bearing systems: An experimental setup approaching fO_2 conditions of natural calc-alkaline magmas. American Mineralogist 90:708-717. https://doi.org/10.2138/am.2005.1663

Le Losq C, Neuville DR, Moretti R, Roux J (2012) Amorphous Materials: Determination of water content in silicate glasses using Raman spectrometry: Implications for the study of explosive volcanism. American Mineralogist 97:779-790. https://doi.org/10.2138/am.2012.3831

Matjuschkin V, Brooker RA, Tattitch B, Blundy JD, Stamper CC (2015) Control and monitoring of oxygen fugacity in piston cylinder experiments. Contributions to Mineralogy and Petrology 169:9. https://doi.org/10.1007/s00410-015-1105-z

van Gerve T, Namur O, Wieser P, Lamadrid H. Hulsbosch N, Neave DA (2021) Constraints on deep magmatic volatile budgets from olivine hosted melt inclusions: Integrating 3D imaging with chemical microanalysis. AGU Fall Meeting 2021 (New Orleans). https://agu.confex.com/agu/fm21/meetingapp.cgi/Paper/891640